

Modeling of Thin Film Solar Photovoltaic Based on ZnO/SnS Oxide-Absorber Substrate Configuration

Anupam Verma* Pallavi Asthana

Department of Electronics and Communication Engineering, Amity School of Engineering and Technology, Amity University, Lucknow, India

Abstract

Due to increasing awareness for using clean energy and therefore greater demand for relying more on the renewable sources which solar photovoltaic are part of because they pose very little or no threat to the environment comparatively, there is growing pressure for reducing electricity generation costs from solar photovoltaic (PV) modules. Hence there is need for alternative new light absorbing materials that can provide conversion efficiencies which would be comparable to the current technologies based on crystalline silicon and CdTe or CIGS thin films at lower manufacturing costs and therefore providing cost effective solutions.

In this paper we have evaluated the tin based absorber material (based on tin monosulfide; SnS) as the next generation of Photovoltaic cells that can provide the desired performance in the long term. Therefore it explores the potential use of tin mono-sulfide as photovoltaic material for conversion of light into electricity. Zinc Oxide (ZnO) thin films have been recognized as good candidates in photovoltaic devices acting as wide-band gap window layer. The results are presented through the numerical analysis done by AMPD-1D simulator tool to explore the possibility of using thin film and stable ZnO/SnS solar photovoltaic device with aim to achieve comparable conversion efficiencies.

A baseline structure of SnS cell was explored in this work with thickness of SnS absorber layer up to 3 μm and .100 μm ZnO layer and showed reasonable efficiencies over 17%. At the end of our research we also suggest that future research efforts in device development should utilize the better suited back contact material (other than the rear metal contact copper that is investigated in this study), so that the efficiency of the device can be enhanced further.

Keywords— SnS, Tin Mono-sulfide, Solar Photovoltaic, Thin Film Solar Cells, AMPS-1D

I. INTRODUCTION

For the solar photovoltaic technology to remain competitive there is the need to reduce the manufacturing costs of the solar photovoltaic modules by almost \$0.50/Wp to \$0.40/Wp i.e. less than half the dollar per unit of the power produced in Watts, Wp and photovoltaic systems by \$1/Wp by 2020[1,2]. At present the most successful thin film technology we have are based on CdTe and CIGS solar photovoltaic light absorbing materials[3]. Due to heavy demand of Tellurium and Indium elemental materials and their limited reserves there is lot of constraint on prices and therefore growing concern about global production and supply trends to sufficiently support the material requirement of the photovoltaic industry and production at reduced costs in future[4]. Since the financial growth of the Photovoltaic industry is dependent on the supply of bankable modules by manufacturers therefore, there is a desire among the material and semiconductor engineers community to find the alternative material choices that can use similar deposition processes and ensure that the processing conditions are not constrained by the limited reserve base or sudden price shocks. Further the \$/Wp cost value can be

reduced either by increasing the efficiencies or by decreasing the production cost.

Keeping this in mind, photovoltaic modelling on a new class of light absorbers based on tin chalcogenide having favourable optoelectronic properties for PV conversion is done and explored to improve the conversion efficiency of the device. This light absorbing material is tin mono sulfide (SnS). Preliminary researches have shown that tin mono sulfide is a sustainable light absorbing material for the photovoltaic devices which is due to its optimum energy band gap and availability in abundance of its raw material as tin and sulfur. Tin mono sulfide (SnS) is a semiconductor with tin in the Sn(II) oxidation state. The reason that SnS is potentially important photovoltaic and solar conversion material is due its direct optical band gap of ~ 1.3 eV[5]. This band gap is similar to silicon and is in the optimum range for solar photo-conversion and therefore the thickness required for the SnS solar cells makes the cost of material relatively low. It is formed from readily available elements and is environmentally benign. In April 2014 the London Metal Exchange reported price of Tin as US \$23100.31/metric-ton which constitutes to around

\$23/kg. This is very low in comparison to Tellurium's \$200/kg price. This favourable price with Tin is due to its much larger global reserves and large annual production. Even if the tin prices were to increase drastically over the next few years, it would still be a relatively tiny fraction of PV manufacturing. The polycrystalline layers of SnS solar cell can be deposited using variety of different low cost techniques such as close space sublimation (CSS), chemical vapour deposition (CVD), chemical bath deposition (CBD) and Atomic layer deposition(ALD) which may be useful for nano meter scale thin film photovoltaic or solar conversion devices[6-8].

II. SOLAR CELL STRUCTURE

The SnS solar cell can be fabricated in a substrate oxide/absorber configuration (see Fig. 1.).

The high efficiency SnS solar cells can be grown in a substrate oxide/absorber configuration where the ZnO/SnS stacks are deposited on an inexpensive glass material which serves as a substrate material. From the application point of view it is the most suitable form for these solar cells. The flexible substrate is at the back of the cell and has to be stable at high temperatures and compatible with the material deposited on it but does not have to be transparent[9].

For the conventional polycrystalline thin film solar cells such as CdTe and CIGS, the fabrication processes requires temperatures of about 450 to 550 degree celcius and this is same with SnS solar cells. Different material layers are deposited on an inexpensive substrate; to form a thin film stack. Glass as a substrate also avoids any temperature issues if any in the deposition scheme. After the processing the cell, a polyimide or a metal foil can be laminated on the back of the device and front glass can be removed by appropriate method which completes the substrate configuration. The advantage with this configuration is also avoidance of absorption losses and possible degradations on the transparency due to UV or electronic and protons irradiation.

substrate configuration

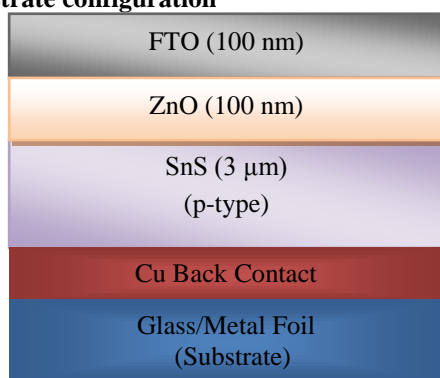


Fig.1. Substrate Configuration for ZnO/SnS Thin Film Solar Cells

This deposition scheme suggests that for the oxide/ absorber configuration, the ohmic contact to the absorber would be initially deposited on glass followed by the 3 μm SnS layer, on top of which the 0.100 μm thick ZnO layer is deposited to complete the n-p hetero-junction formation. To minimize optical absorption losses from the ZnO surface by reflection and maximize collection of photo-generated electrons from the oxide, a 0.100 μm TCO layer of Fluorine doped tin oxide (FTO) is used as part of the model structure. Copper is used as a real metal contact of 0.250 μm thickness so as to withstand the mechanical stresses caused by the overlaying materials so that the integrity of the absorber contact interface is not compromised for photovoltaic performance over the course of the device life time. Reason for choosing hetero junction solar cell structure is because they have potentially higher efficiency than their homo junction counterparts and are less affected by operating temperatures. ZnO is considered as an excellent complement to SnS here because of its wide band gap (~3.35 eV), high free carrier concentrations for electron conduction ($1.0\text{E}18 \text{ cm}^{-3}$), and very similar electron affinity (4.35 eV) to SnS. These properties suggest minimum voltage losses during charge transport across the interface. The oxide forms a chemically stable p-n hetero junction such that the photo generated electrons (minority carriers) from the absorber can be collected effectively and transported to their respective contacts with minimal current losses. Also low toxicity and relatively easy processing of ZnO makes it an attractive proposition for large scale utilization with SnS[10]. The device utilizes 0.25 μm F doped SnO₂ i.e Fluorine doped tin oxide (FTO) as the transparent conductive oxide (TCO), on which a 0.25 μm layer of ZnO having wide band gap serves as the window material that forms the Schottky barrier with the 3 μm thick absorber SnS. Copper is used as the metal forming the ohmic contact at the rear end and its thickness is not a consideration that effects photovoltaic behaviour. ZnO serves as a 'window' layer as explained that transmits most of the visible band solar irradiance to the underlying SnS absorber material.

III. INPUT PARAMETERS

A. Front and Back Contacts

Generally, contacts can be assumed ohmic or, depending on the focus of the modelling, assigned a Schottky barrier height consistent with experimental observations. The reflection at the back surface has only minor influence on the achievable short-circuit current density (J_{sc}), and these influences only become noticeable if the absorber is chosen to be fairly thin. Most of the modelling tools support a constant multiplicative reflection factor for the front

surface (i.e Rf = 0.1, 10% reflection). Quantum efficiency (QE) is then reduced by this fraction and, if interference effects are neglected, Quantum Efficiency will show a fairly flat response at intermediate wavelengths of ~1-Rf [11].

At the front we have FTO/ZnO interface which forms schottky contact since ZnO is a n-type semiconductor and has work function lower than that of FTO which makes a case for Schottky or rectifying contact for the n-type semiconductor and metal contact. Barrier height of such contact, ϕ_f can be calculated by subtracting electron affinity, χ_s of ZnO from the work function of metal, ϕ_m which in this case is FTO. At the back we have SnS/Copper contact which forms an ohmic contact since SnS is a p-type semiconductor which has lower and closer work function relative to the metal which is Copper. Therefore this becomes the case of ohmic contact for the p- type semiconductor and metal contact. Barrier height, ϕ_b of such contact can be calculated as [$E_g - (\phi_m - \chi_s)$], where E_g is the optical energy band gap of the semiconductor[12].

B. Material Properties

The carrier mobility for the polycrystalline material should be chosen lower than the values reported for the crystalline material[11]. Effective masses of carriers for SnS is $m_e^* = 0.50m_0$ (Vidal et. al 2012) for electrons and $m_h^* = 0.11m_0$ (Reddy and Reddy 2006) for holes. The electron and hole mobility are 100 cm²/V-sec and 25 cm²/V-sec respectively. The dielectric constant for SnS is 16(Chandrasekhar et. al 1977). Electron affinity, χ is 4.20(B. Subramanian et. al. 2001). For ZnO, $m_e^* = 0.29m_0$ for electrons and $m_h^* = 0.21m_0$ for holes. Electron and hole mobility for ZnO are 100 cm²/V-sec and 20 cm²/V-sec respectively. Dielectric constant for ZnO is 9 and for FTO it is 10[13].

The effective density of states, Nc for conduction band can be calculated using equation. (1) and similarly Nv for valence band using equation (2)[14]. The direct temperature dependence in Nc and Nv should be taken into account for temperature dependence modelling.

$$N_c = 2 \left(\frac{2\pi m_e^* KT}{h^2} \right)^{\frac{3}{2}} \tag{1}$$

$$\text{and } N_v = 2 \left(\frac{2\pi m_h^* KT}{h^2} \right)^{\frac{3}{2}} \tag{2}$$

where K,T and h are Boltzmann's constant, ambient temperature and Planck's constant respectively. Free carrier concentration, energy band gaps and other material properties are listed in table I.

TABLE I
 OPTOELECTRONIC PROPERTIES OF MATERIALS USED IN MODELLING

Optical Parameters	Semiconductor Material		
	SnS	ZnO[13]	FTO[13]
Eg (eV)	1.30	3.35	3.8
Conductivity Type	p	N	n
Nc (cm ⁻³)	8.9 × 10 ¹⁸	3.9 × 10 ¹⁸	1.2 × 10 ²⁰
Nv (cm ⁻³)	1.0 × 10 ¹⁸	2.4 × 10 ¹⁸	7.0 × 10 ²⁰
χ (eV)	4.20	4.35	4.50
μ _n (cm ² /V-sec)	100	100	100
μ _h (cm ² /V-sec)	25	20	20
Free carrier concentration (cm ⁻³)	7.4 × 10 ¹⁶	1.0 × 10 ¹⁸	3.5 × 10 ²⁰
Dielectric Constant	16	9	10

C. Absorption Profile

The ability of an absorber to absorb light of different wavelengths is defined by its absorption coefficient 'α' that is a function of wavelength lambda (λ). Beer-Lambert's law is applied to calculate the absorbance A relative to the incident flux intensity (photons impinging per cm² per second), some of which is reflected off the material surface on which it is incident (always referred to as the "front" end) and some transmitted (T) so that light emerges from the opposite side (always referred to as the "back" end) of the material.

Based on this law, the absorbance A is a function of lambda (λ) which is given by[15]:

$$A(\lambda) = [1 - R][1 - \exp(-\alpha(\lambda)d)] \tag{3}$$

where d is the thickness of the material traversed by the light radiation and R is the reflectance.

It is seen from the above equation that absorption increases exponentially with 'α' or the material thickness 'd'. It is therefore desirable to use thick material layers and/or semiconductors that have high absorption coefficients so that the value A can be maximized. The absorption length in the labs is a quantity used to denote absorption characteristics, and is defined as the thickness required to absorb 63% of the impinging light or equivalently required to develop 63% of the potential, Jsc available. This value corresponds to the "α.d" product equalling '1' in the exponent of above equation, so the absorption coefficient may be defined as the reciprocal of the absorption length, and vice versa. The absorption profile was calculated from the works of Brownson et. Al [16]. The absorption profiles are calculated as a

function of wavelength λ for different materials employed in the structure.

IV. RESULT AND DISCUSSION

With the objective to model baseline tin-based structures, no intermediate gap states having discrete or Gaussian distribution of energy levels are considered or assumed. The research corresponds to constant cell operating temperature of 300K or the ambient temperature along with studying the performance of optoelectronic structures under illumination, voltage biasing has been considered or its influence evaluated. For a general baseline cell structure with FTO/ZnO/SnS/ thickness as 100 nm, 100 nm and 3 μm respectively the short circuit current density, J_{sc} of 26.236 mA/cm^2 ; Open circuit voltage, V_{oc} of 0.759 Volts and 85% Fill Factor was achieved which yielded conversion efficiency, η of about 16.165%.

With the aim of achieving an optimized conversion efficiency, we experiment and observe the results by manipulating the width and doping concentration of the oxide and absorber layers in a sequential manner. We start by observing if FTO has any influence on the cell output characteristics with variations in its doping or width and as expected there were no change in the cell's output characteristics. Same was the case with variations in width of the ZnO. Therefore the standard width of 100 nm each for both FTO and ZnO were considered along with their doping or free carrier concentration.

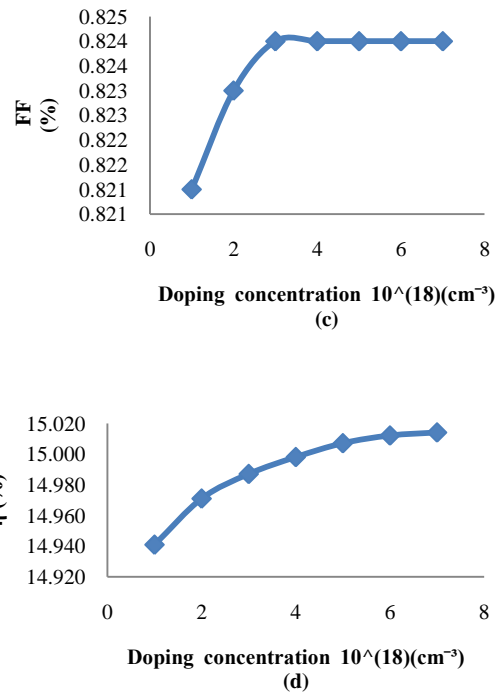
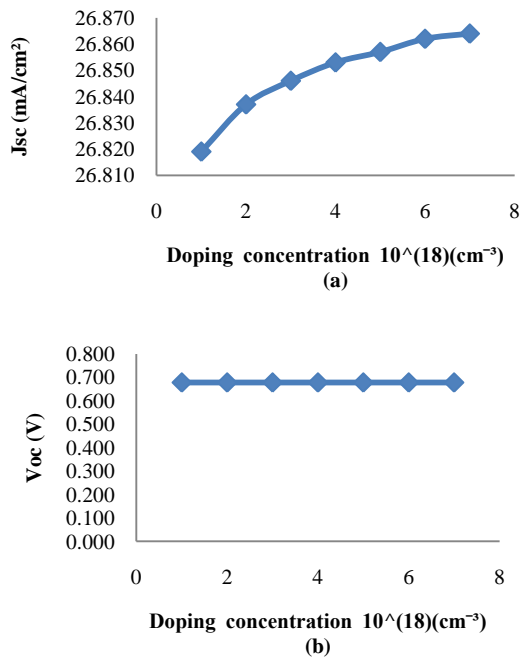


Fig. 2. Impact of Variations in Doping Concentration of ZnO on Cell's output characteristics: (a) Short Circuit current Density, J_{sc} (b) Open circuit voltage, V_{oc} (c) Fill Factor, FF and (d) conversion efficiency, η

However for ZnO variations in its doping concentration resulted into changes in the cell's output characteristics as shown in Fig. 2. From this figure we observe that there is increase in the short circuit current density J_{sc} , as the doping concentration is increased up to $7.00\text{E}+18 \text{ cm}^{-3}$ beyond which it starts to saturate and has no effect on further increase. Open circuit voltage remains same on increasing the doping concentration but the fill factor rises with little increase (up to $4.00\text{E}+18 \text{ cm}^{-3}$) in concentration and remains unchanged for the rest of it. Consequently, the conversion efficiency, η rises non linearly for the increase up to $7.00\text{E}+18 \text{ cm}^{-3}$ and has a very minute change after that. With these observed results we take optimized value of doping concentration for ZnO as $7.00\text{E}+18 \text{ cm}^{-3}$ and use it to further observe the impact on cell's output characteristics for variation in width of SnS as shown in Fig. 3.

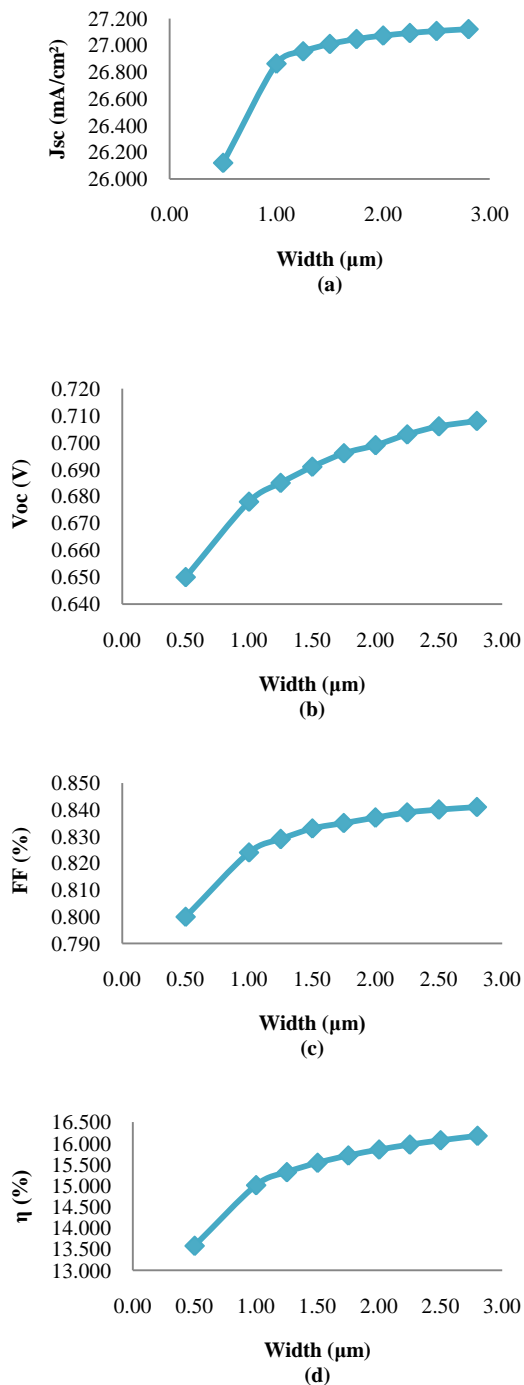


Fig. 3. Impact of variations in width of SnS on cell's output characteristics: (a) Short circuit current density, J_{sc} (b) Open circuit voltage, V_{oc} (c) Fill factor, FF and (d) Conversion efficiency, η

It is evident from the Fig. 3. that the short circuit current density increases with increase in width of absorber layer of SnS up to ~3 µm. It is also seen that beyond 1 µm decrease in width there is sharp fall in short circuit current density, J_{sc} . Therefore width of SnS absorber layer should at least be greater than 1 µm. Almost a similar increase is seen in open circuit

voltage as for short circuit current density, J_{sc} and fill factor, FF. Conversion efficiency, η rises in a similar manner, non linearly and continues as in case of J_{sc} and therefore we have final absorber layer width as 3 µm as optimal width and use it to explore impact on cell's output characteristics with variations in SnS doping concentration.

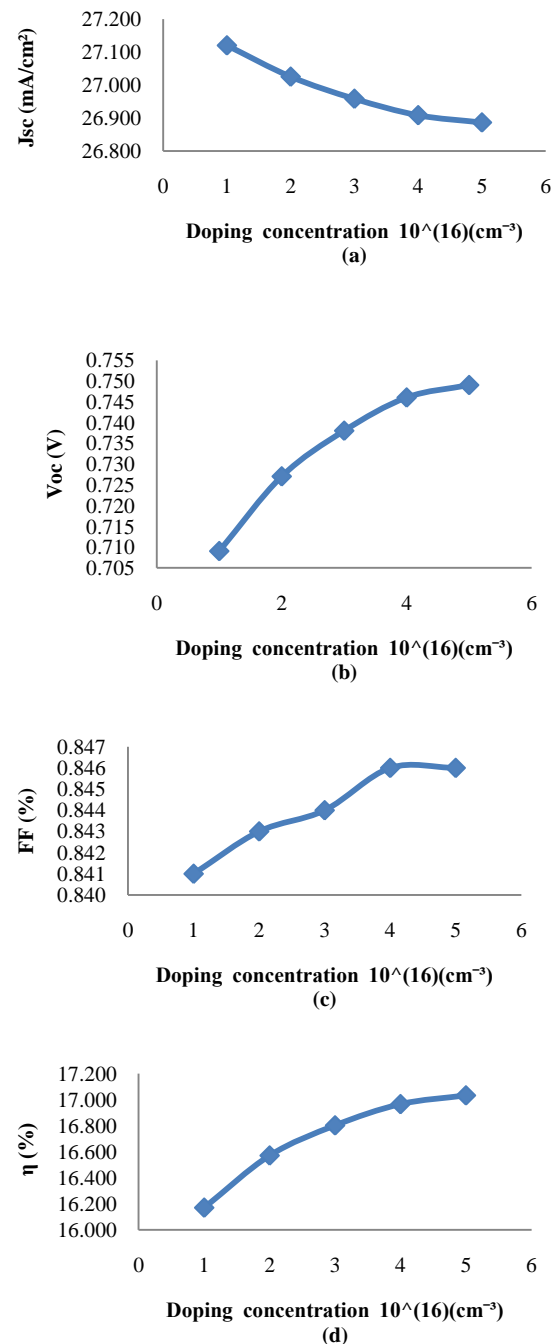


Fig. 4. Impact of variations in doping concentration of SnS on cell's output characteristics: (a) Short circuit current density, J_{sc} (b) Open circuit voltage, V_{oc} (c) Fill factor, FF and (d) Conversion efficiency, η

Fig. 4. shows effect of doping variations in absorber layer, SnS. We observe there is a fall in short circuit current density, J_{sc} on increasing the doping concentration in SnS as it falls from 27.125 mA/cm² to 26.825 mA/cm² when doping is increased as shown in Fig. However there is increase in the open circuit voltage, V_{oc} and Fill Factor, FF and hence the increase in conversion efficiency, η to 17.032%. The final cell output characteristics achieved are $J_{sc} = 26.868$ mA/cm², $V_{oc} = 0.749$ V and FF = 84.6%. Energy band diagram and Electric field for the photovoltaic are shown in Fig.5 and Fig.6 respectively.

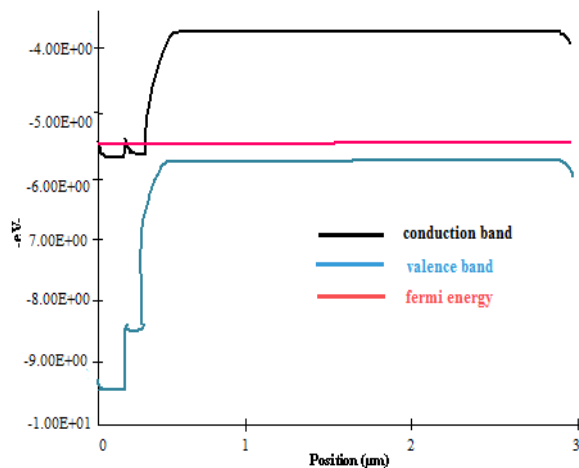


Fig. 5. Energy Band Diagrams for ZnO/SnS thin film solar photovoltaic at thermodynamic equilibrium.

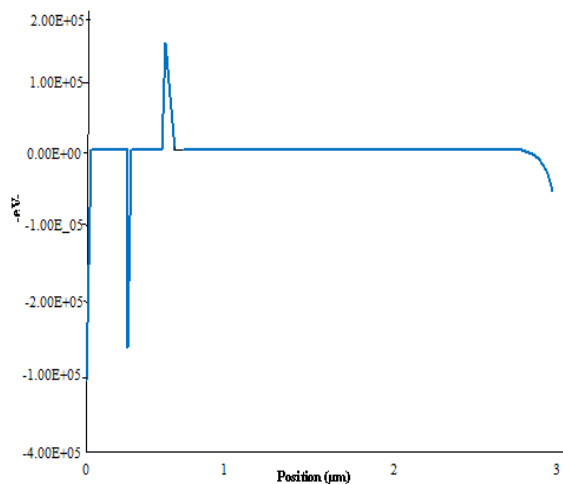


Fig. 6. Electric field Vs. position for ZnO/SnS thin film solar photovoltaic. for light ON, $V=0$.

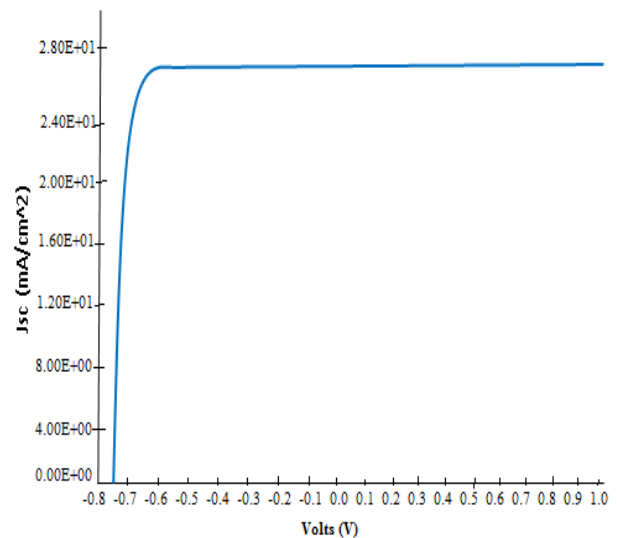


Fig. 7. Final J-V characteristic plots for ZnO/SnS thin film solar photovoltaic.

Final J-V characteristics plot is shown in Fig. 7. The plot is shown for the values of barrier heights for front contact, ϕ_f and back contact, ϕ_b of 0.90 eV and .10 eV respectively. Assuming sufficiently high bulk recombination, the net forward current becomes limited below V_{oc} . The manipulations/variations in the parameters of the layers result into increase of conversion efficiency, η from the initial value of 16.165% to 17.032%, an increase of 5.4%. If a superior metal to copper is used as a rear metal contact for this PV device, further improvement in the efficiency can be achieved since the use of copper due to economic constraints causes reverse electron current into the metal because of undesirable band energy equilibrium. This causes fermi level splitting between electrons and holes to narrow down at the interface, which reduces the open circuit voltages. Use of platinum as an ohmic contact to this device supports higher voltage due to favourable band alignments and also resolves negative current issue observed earlier.

V. ACKNOWLEDGMENTS

The modelling and calculation of this work used the AMPS software developed at the Pennsylvania State University by S. Fonash et al. and supported by the Faculty Members Dr. Geetika Srivastava and my Guide Sr. Lec. Ms. Pallavi Asthana at Amity University, Lucknow.

REFERENCES

- [1] David Feldman, Robert Margolis, Ted James and Alan Goodrich, *Photovoltaic System Pricing Trends: Historical, Recent and Near-Term Projections*, 3rd ed., NREL, US Department of Energy, 2013.
- [2] "SunShot Initiative: Solar Program Highlights", U.S. Department of Energy,

- Washington,DC, <http://www1.eere.energy.gov/solar/sunshot/highlights.html>, accessed 8th Feb, 2013
- [3] Ayodhya Nath Tiwari, *Advances in Thin Film PV: CIGS and CdTe, Towards High Efficiency and Cost Reduction Concepts*, Laboratory for Thin Films and Photovoltaics, Empa-Swiss Federal Laboratories for Material Science and Technology, Dübendorf, Switzerland, June 2013
- [4] Vasilis Fthenakis, *Sustainability Metrics for Extending Thin Film Photovoltaic to Terawatt Levels*, Material Research Society Bulletin, Vol 37, 2012.
- [5] Julian Vidal; Stephan Lany; Mayeul d'Avezac; Alex Zunger; Andriy Zakutayev; Jason Francis and Janet Tate, *Band Structure , Optical Properties and Defect Physics of the Photovoltaic Semiconductor SnS*, Applied Physics Letters, Vol. 100, 3rd ed., Jan. 2012.
- [6] N Sato; M Ichimura; Y Yamazaki and E Arai, *Characterization of electrical Properties of SnS Thin Films Prepared by the Electrochemical Deposition Method*, Proceedings of 3rd World Conf. on Photovoltaic Energy Conversion, IEEE, Vol. 1, p 38-41, Japan, May.2003
- [7] J.B. Johnson; H Jones; B.S. Latham; J.D. Parker; R.D. Engelken and C Barber, *Optimization of Photoconductivity in Vacuum Evaporated Tin Sulfide Thin Films*, Semicond. Sci. Technol., IOPScience, Vol 14, p 501-507, 1999.
- [8] Jay Yu Kim and Steven M. George, *Tin Monosulfide Thin Films Grown by Atomic Layer Deposition Using Tin 2,4-Pentanedionate and Hydrogen Sulfide*, High and Low Concentrator Systems for Solar Electric Applications, SPIE Proceedings Vol. 7769, Aug. 2010.
- [9] I. Matulionis; S. Han; J.A. Drayton; K.J. Price and A.D. Compaan, *Cadmium Telluride Solar Cells on Molybdenum Substrates*, MRS Spring Proceedings, San Francisco, H8.23, p.1-4, 2001
- [10] Jerome Steinhauser, *Low Pressure Chemical Vapor Deposited Zinc Oxide for Thin Film Silicon Solar Cells: Optical and Electrical Properties*, Institute of Microtechnology, University of Neuchatel, Switzerland, Nov. 2008
- [11] M Gloeckler; A.L. Fahrenbruch and J.R. Sites, *Numerical Modeling of CIGS and CdTe Solar Cells: Setting the Baseline*, Proceedings of 3rd World Conf. on Photovoltaic Energy Conversion, IEEE, Vol. 1, p. 491-494, Japan, May 2003.
- [12] M. Balkanski and R.F. Wallis, *Semiconductor Physics and Applications*, Condensed Matter Physics, Oxford Univ. Press, 2000.
- [13] B. Subramanian, C. Sanjeeviraja, M. Jayachandra, *Cathodic Electrodeposition and Analysis of SnS Films for Photochemical Cells*, Mat. Chem. and Phys., Vol. 71, pp. 40-46, 2001
- [14] S.M. Sze, *Physics of Semiconductor Devices, 2nd Edition*, John Wiley & Sons, New York, 1981
- [15] S.J. Fonash, *Solar Cell Device Physics*, 2nd Ed. Elsevier, USA, 2010.
- [16] J.R.S. Brownson; C Georges and C.L. Clement, *Synthesis of a δ -SnS Polymorph by Electrodeposition*, Chem. Mat. Vol. 18, p. 6397-6402, 2006.